Turkish Journal of Electrical Engineering & Computer Sciences

http://journals.tubitak.gov.tr/elektrik/

Research Article

Turk J Elec Eng & Comp Sci
(2016) 24: 355 – 369

doi:10.3906/elk-1210-37

Kernel Fisher discriminant analysis of Gabor features for online palmprint verification

Murat EKİNCİ*, Murat AYKUT
Computer Vision and Pattern Recognition Lab., Karadeniz Technical University, Trabzon, Turkey

Received: 08.10.2012 • **Accepted/Published Online:** 04.08.2013 • **Final Version:** 05.02.2016

Abstract: We propose an online palmprint identification and verification algorithm with the use of kernel Fisher discriminant analysis (KFD) on the Gabor wavelet representation of palm images. Desirable palm features are derived by Gabor wavelets on the palm region. The KFD method is then employed to extract higher order relations among the Gabor-palm images for palmprint recognition. As a real-world application, the proposed algorithm was adapted into a novel online palmprint verification system that was employed in a student laboratory for 3 months. The feasibility of the Gabor-based KFD method was successfully tested on our proposed online palmprint system and on two data sets: KTU database, acquired in this real-life application, and the PolyU database. Comparing with existing PCA, KPCA, and Fisher discriminant analysis, the proposed method gives superior results on the KTU palmprint database. Furthermore, for palmprint recognition, our approach provides highly competitive performance (99.714% recognition rate and 0.078% equal error rate) with respect to the published palmprint recognition approaches tested with the same scenario on the public PolyU database.

Key words: Biometrics, online palmprint verification system, kernel Fisher discriminant, Gabor wavelet, palmprint application in real world

1. Introduction

The palmprint has attracted increased interest in biometrics [1]. Palmprint recognition inherently implements many characteristics in a palm region called the palmprint pattern. Palmprint patterns have uniqueness and permanence; they also require minimum cooperation from the user. This work has two main novelties: a complete online palmprint identity verification system that includes necessary hardware and software, and a Gabor-based kernel Fisher discriminant (KFD) method for palmprint recognition. Palmprint recognition systems given in the literature can be divided into two categories, according to the sensors: scanner-based [2] and camera-based [3]. Scanner-based systems require less effort for the system design, but the scanning time is not short enough to support real-time video access. Camera-based systems give better results with proper selection of lens, camera, and light sources. Therefore, we preferred to use a low resolution CCD camera for capturing palm images. The previous palmprint verification/authentication systems in [3–5] were used for database acquisition in laboratory conditions. There was a human administrator telling the user what to do. The images were also collected in one or two sessions. In both sessions, the users placed their hands regularly. However, for the verification experiments, this regularity is far from real-world conditions. In the present work, the proposed palmprint verification system was deployed at the entrance to a student laboratory for

*Correspondence: ekinci@ktu.edu.tr

access control. The system is able to capture hand images, and can open a door when the user is positively verified. While our system was utilized for 3 months, hand and palmprint images were simultaneously stored in a database that can be used for developments related to existing and considering algorithms. Therefore, the palmprint samples in our database were collected from real-world applications. In these applications, the system was autonomous and the individuals did not get any guidance from a human supervisor on how to use the system. The numbers of sample images per user and the time interval between acquisitions were different for each user. Since the system was employed in daily usage, the users also made their verification attempts on the system at various times. Moreover, some unregistered users performed biometric attacks (attempt to be recognized as another user) during database acquisition. That is, some students claimed to be another user by presenting their hands while giving a noncorrect ID number. Consequently, the images in our dataset can also be utilized to achieve more realistic experiments for palmprint verification studies.

Another main contribution of this paper is to propose a nonlinear feature extraction method for palmprint recognition. In the literature there are mainly three types of palmprint recognition approaches: local feature-based [3,6,7], holistic-based [8–10], and hybrid [11]. Local feature-based methods extract local salient features from palmprint images and use a matcher to compare these against stored templates. Line-based, coding-based methods, and local texture descriptors are included in this group. Holistic-based methods treat a palmprint image as an image, a high dimensional vector, or a second rank tensor, and feature extraction and classification techniques are then used for palmprint recognition. Subspace methods (also called appearance-based methods), invariant moments, and spectral representation are three main subclasses of this type of feature extraction method. The appearance-based methods utilize feature extraction methods like PCA, LDA, or LPP, and can be used with some image representation methods representing the images in a spatial or a transform domain. Hybrid methods also use both holistic and local features to improve the recognition accuracy or facilitate identification speed [12].

In the proposed appearance-based method, owing to the robustness against local distortions, Gabor wavelets are firstly used to derive palm features characterized by spatial frequency, spatial locality, and orientation selectivity. Then the KFD method [13] is utilized to project the palmprints from the high dimensional Gabor palmprint space to a significantly lower dimensional feature space in a nonlinear manner, which allows a good discrimination between different palms. Finally, a weighted Euclidean distance-based nearest neighbor classifier is employed for matching and classification. The feasibility of the proposed algorithm has been successfully tested on both the KTU [14] and PolyU [3] (which is commonly used in the literature) palmprint databases.

In palmprint biometrics, a 2D Gabor filter was used first to utilize zero-crossing information on a palmprint image to have a texture called PalmCode [3]. Subsequently, Sun et al. [5] used Gabor filters to generate ordinal feature codes by producing orthogonal line ordinal features for palmprint representation. In [15] and [16], Gabor feature-based $(2D)^2$PCA and kernel PCA (KPCA), respectively, were proposed for palmprint recognition. In a recent work [17], a Gabor filter bank was also analyzed for palmprint recognition. Fisher discriminant analysis was also used to represent palmprint features in some early works [18–21]. In [18,19], linear discriminant analysis was used for palmprint feature extraction. Kernel Fisher discriminant analysis was also applied on raw palmprint images simply, to represent features, in [20]. In [21] the palmprint features were also extracted by using a Gabor filter and linear Fisher discriminant analysis. In the present paper, unlike the above studies, kernel Fisher discriminant analysis integrated with a Gabor wavelet representation of the palm images is proposed. The radial basis function (RBF) kernel and 1vsA output coding scheme are used to achieve the kernel Fisher

analysis. The proposed algorithm was also coded with C++ programming language and employed in an online palmprint verification system. This system was successfully employed for user verification access control in a normal office (a PC lab for students in our department) environment.

The rest of the paper is organized as follows: Section 2 introduces our online palmprint verification system, briefly. The proposed feature extraction method is detailed in Section 3. Experimental results to show the system performance are achieved on our palmprint database acquired from real-world biometric applications and the PolyU palmprint database. Those results are comparatively discussed in Section 4. The conclusion is finally presented in Section 5.

2. Online palmprint biometric system

Our palmprint-based identity verification system consists of the following components: (1) a standard PC with Intel Core2 Quad CPU, 4 GB RAM, 500 GB HD, and Windows Vista operating system; (2) a wire resistive touch panel mounted on a CRT display, which forms a touch screen, for practical user-system interaction with no keyboard; (3) a low cost CCD camera with a DC auto iris lens that has 28 mm focal length, maximum aperture of f/2.8, and wide angle of vision for viewing the hand region completely (exposure and focus adjustments were made for the best image quality); (4) 6500° K white LED-based lighting sources placed at a certain angle (35 degrees for the upper LEDs and 70 degrees for the lower LEDs), which improve the image quality and reveal the details in the palm image; (5) a hand placement platform designed for convenient hand placement, stable imaging, and minimum effects from the illumination changes at the outside; (6) an electrical door lock; (7) an electronic controller interface circuit connected to the PC via a serial port, which controls door opening, CCD cameras, and light sources. The external view of the system is shown in Figure 1.

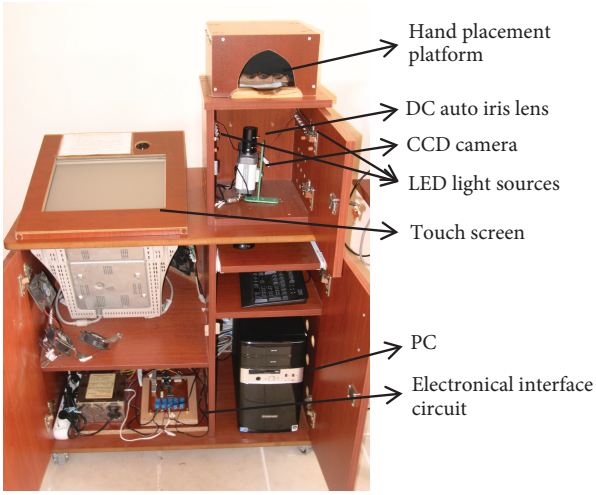

Figure 1. External view of our palmprint verification system.

The online palmprint verification system was located at a student PC laboratory for access control[1]. In this task, the user touches the screen and then enters her/his identity number. Next, the lighting source is turned on and the frame grabbing process is automatically initialized. The image resolution is selected as 768 × 576 pixels at 75 dpi, taking account of the trade-off between the qualities of the images, which reveals

[1]A demo video of the online system can be watched at: http://youtube.com/watch?v=TI7QjkabCXQ

the details of the palm texture, and fast processing, which is necessary for online systems. If the system does not detect a hand placed into the platform within a certain time, the lighting source is turned off and the CCD camera is deactivated for system safety and energy saving. When an object in the scene is detected and then recognized as a stationary hand by comparing its size and shape, the whole palm and palmprint images automatically extracted by using an algorithm are then stored in a database.

Figure 2a depicts the appearance of a palmprint, called the region of interest (ROI) of the palm. A user-friendly interface screen is shown in Figure 2b, when the user has presented her/his hand. The green curves are used to guide how the users should place their hands into the platform. The text shown in the image is a message and says "*Place your hand into the system*". A square drawn with red lines, as shown in Figure 2b, is positioned on the image to indicate the ROI of the palm. Figure 2c also shows a subimage (palmprint image) extracted from the whole palm image.

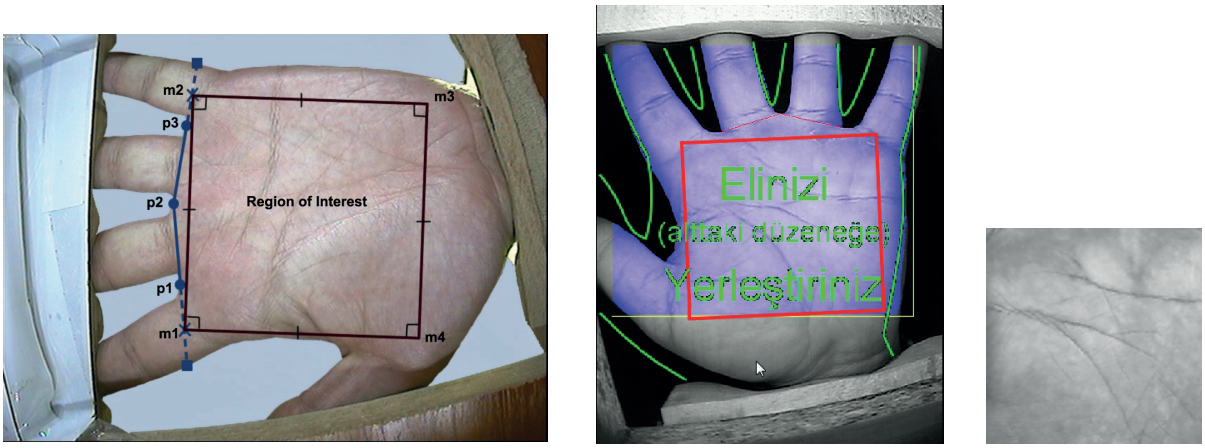

(a) (b) (c)

Figure 2. a) Outline of the region of interest (ROI) extraction from a palm. b) An original image is shown, while the online system depicts the central part of a palm by drawing a square shape with red lines. c) The extracted palmprint image from a real-life application.

The users made the enrollment and verification attempts on the system without a human supervision. In the enrollment task, the frame grabber is activated to grab the hand image and to select the ROI of the palm, as a first training sample. Subsequently, it is requested from the user to take out her/his hand from the platform and then re-present her/his hand (in a reasonable amount of time). This is only repeated at the enrollment stage to collect four palm images from each user for a training set. If the user does not replace her/his hand in the required time (it is assigned as 5 s in this real work), the system will go to the initial state. In each attempt, the whole palm and the extracted palmprint images (ROI), as shown in Figures 2b and 2c, are saved in both enrollment and verification stages for constituting a palmprint database.

In the verification stage, the users first enter their identity numbers and then present their hands to the platform. The palmprint image is extracted by selecting the ROI of the palm image. The palmprint image representation (pattern) is generated by using discrete transforms and feature extraction methods as explained in Section 3. Then the generated pattern is matched with the related individual's patterns in the database. If the maximum similarity (or minimum distance) is higher than the predefined threshold, it is accepted as genuine and the door is opened via the electronic interface. Otherwise, the palm image is saved as unrecognized

samples. Simultaneous to system operation, all experiments and events are registered in log files. Figure 3 shows the main flow of the system. All of the enrollment and verification phases are automatically realized on the online system in the real-world conditions.

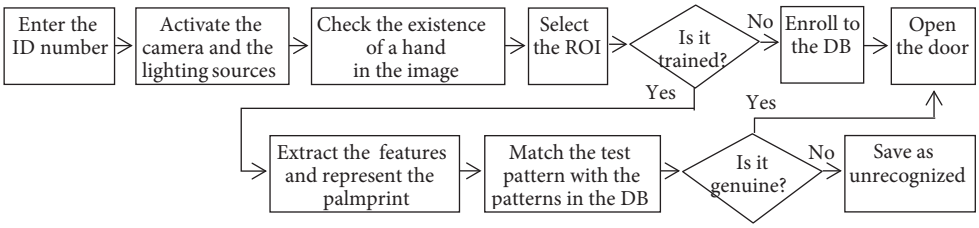

Figure 3. Work flow of our palmprint verification system.

3. Preprocessing

The grabbed image contains a hand object and background, as shown in Figure 2a. To segment the hand from the background, Otsu's thresholding technique [22] is applied. The ROI, a smaller region from the central part of a palm image, is automatically extracted by using the method explained in [2]. In this approach, to locate the ROI, the gaps between the fingers are used as reference points. As shown in Figure 2a, the boundaries of the gaps between the fingers are extracted and then the valleys of the fingers, p_1, p_2, p_3, are obtained by using a border tracing algorithm [23]. Based on those valley points, two valley points, p_1 and p_2, are connected to form a reference line to intersect the right edge of the hand. This intersection and p_1 points are used to compute the midpoint, m_1. This is repeated to find the other midpoint, m_2, by using the points p_2 and p_3. To obtain one of the edges for a geometrical square shape, the two midpoints, m_1 and m_2, are connected. Then a square shaped ROI is extracted as shown with black lines drawn in Figure 2a and with red lines drawn in Figure 2b. The size of the square is automatically resized to 128 $\times$ 128 for representing the palmprint patterns for further processing. A resized pattern is shown in Figure 2c.

4. Palmprint representation

4.1. Gabor wavelet feature representation

As the first step of the feature extraction, we propose to use Gabor wavelets due to their optimal localization properties in both spatial and frequency domains [24]. Their importance is increased by biological relevance [25], and therefore they have been widely applied to texture segmentation [26] and face recognition [27].

In Gabor wavelets, the basis function is a Gabor kernel, which is a Gaussian modulated by a complex sinusoidal:

$$g(x,y) = \left(\frac{1}{2\pi\sigma_x\sigma_y}\right)\exp\left[-\frac{1}{2}\left(\frac{x^2}{\sigma_x^2}+\frac{y^2}{\sigma_y^2}\right)+2\pi jWx\right], \tag{1}$$

where σ_x and σ_y are the horizontal and vertical standard deviations of the Gaussian envelope, and W is central frequency. Then Gabor wavelets can be achieved with dilation and rotations of this kernel:

$$g_{mn}(x,y) = a^{-m}g(x',y'), \quad a>1, \tag{2}$$

$$x' = a^{-m}(x\cos\theta + y\sin\theta), \;\; y' = a^{-m}(-x\sin\theta + y\cos\theta), \tag{3}$$

where $\theta = \mathrm{n}\pi/\mathrm{K}$, a^{-m} is the scale factor, and K is the total number of orientations.

In this work, the Gabor feature representation of a palm image is achieved by convolving the set of Gabor kernels obtained by selecting different orientations and scales. In our approach, to reduce the computational cost for palmprint representation, five different scales and four orientations of Gabor wavelets $\mathrm{S} = \{\ \mathrm{g}_{mn}(\mathrm{x,y}) : \mathrm{m} \in \{0,\ldots,3\}\ ,\ \mathrm{n} \in \{0,\ldots,4\}\ \}$ were used. Gabor function parameters (lower and upper center frequencies) were selected as $\mathrm{U}_{low} = 0.2$ and $\mathrm{U}_{high} = 0.5$, empirically. To make it more robust against brightness changes, DC coefficients of the filters were also removed.

4.2. Kernel Fisher discriminants (KFD)

KFD has been found very effective in many real-world biometric applications [1]. The KFD seeks to solve the well-known Fisher linear discriminant (FLD) problem in a nonlinear feature space.

Let $\{x_i | i = 1, ..., \ell\}$ be the training sample and $y \in \{-1, 1\}^{\ell}$ be the vector of corresponding labels. FLD aims at finding the best separation hyperplane via maximizing the between-class variances and minimizing the within-class variances. This can be achieved by maximizing the Rayleigh coefficient:

$$J(w) = \frac{w^T S_B w}{w^T S_W w}, \tag{4}$$

where

$$S_B = (m_2 - m_1)(m_2 - m_1)^T$$
$$S_W = \sum_{k=1}^{2} \sum_{i \in I_k} (x_i - m_k)(x_i - m_k)^T$$

Here m_k and I_k denote the mean vector and the index set of the class k, respectively. To formulate the problem in high-dimensional nonlinear feature space with the kernel manner, usage of the training samples must be converted in terms of dot-products. Using some algebra, the optimization problem for the KFD in the feature space can be written as [13]

$$J(\alpha) = \frac{\left(\alpha^T \mu\right)^2}{\alpha^T N \alpha} = \frac{\alpha^T M \alpha}{\alpha^T N \alpha} \tag{5}$$

where $\mu_i = 1/\ell_i K\, 1_i$, $\mu = \mu_2 - \mu_1$, $M = \mu\mu^T$, $N = KK^T - \sum_{i=1,2} \ell_i \mu_i \mu_i^T$, $K_{ij} = k(x_i, x_j)$, and k is the kernel function. When the dimension of feature space is higher than that of the training samples, some form of regularization is necessary. It is accomplished by adding an identity or kernel matrix to matrix N.

To maximize the Rayleigh coefficient, the solution of the eigenproblem $M\alpha = \lambda N \alpha$ is recommended. However, for large number of samples the solutions are nonsparse. For this purpose Mika et al. [28] proposed to use a convex quadratic programming problem:

$$\min_{\alpha, b, \xi} \|\xi\|^2 + CP(\alpha) \tag{6}$$

subject to:

$$K\alpha + 1b = y + \xi \tag{7}$$

$$1_i^T \xi = 0, \quad i = 1, 2 \tag{8}$$

Here α, ξ are ℓ dimensional vectors, and b, C are scalar real numbers, $C \geq 0$. P is a regularizer and the term $\|\xi\|^2$ minimizes the variance of the error. The first constraint pulls the outputs of each sample to their class and the second ensures that the average outputs for each class are the label. The KFD features for the test sample x are computed by:

$$(w \cdot \Phi(x)) = \sum_{i=1}^{l} \alpha_i k(x_i, x) \tag{9}$$

The KFD explained above is a binary problem and can be easily extended to multiclass problems. The most widely used techniques are one-versus-all (1vsA) and one-versus-one (1vs1) output coding. In our experiments we used RBF kernel and 1vsA output coding due to the less overhead than 1vs1 coding.

4.3. Similarity measurement

Weighted Euclidean distance (WED) [29] has been chosen for measuring similarity instead of standard Euclidean distance due to performance improvement. It is defined as follows:

$$d_k = \left(\sum_{i=1}^{N} \frac{(f(i) - f_k(i))^2}{(s_k)^2} \right)^{1/2}, \tag{10}$$

where f and f_k are the feature vectors of the test and k-th train patterns; s_k and N denote its standard deviation and vector length.

5. Experiments and results

We evaluated the performance of the proposed method on the KTU [14] (acquired in this work) and the PolyU-II (commonly used in the literature) palmprint databases.

5.1. KTU palmprint database

We acquired a database containing 2043 images from 337 individuals with a novel online palmprint verification system deployed at a student laboratory entrance for 3 months [14]. The palmprint images were collected by using a low cost CCD camera with resolution of 768 $\times$ 576 pixels at 75 dpi. The number of samples per individual in the database was restricted between 4 and 20. The images were gathered on separate occasions (average occasion per class is 3.4), because the samples were provided from real-life applications. There were realistic variations in the images such as focuses, illuminations, and pose of the hand. At the enrollment and verification stages, the users were automatically guided by the system employed in the real environment.

On the first occasion, which is defined as the enrollment stage, the user was automatically asked to enter her/his identity number and then to provide 4 images from the right hand. In the verification (test) stage, the subject first enters her/his identity number via touchless screen, and then s/he is asked to place her/his hand into the platform. To achieve a user-friendly palmprint verification system, a few instructions are given to the subjects via a screen during system usage. This gives us an opportunity to get a novel palmprint database acquired from the system employed in real-life conditions. Some user carelessness such as stained hands and clothes overlapping hands happened during the collection period for the palmprint images. Some variations that occurred in the patterns are shown in Figure 4.

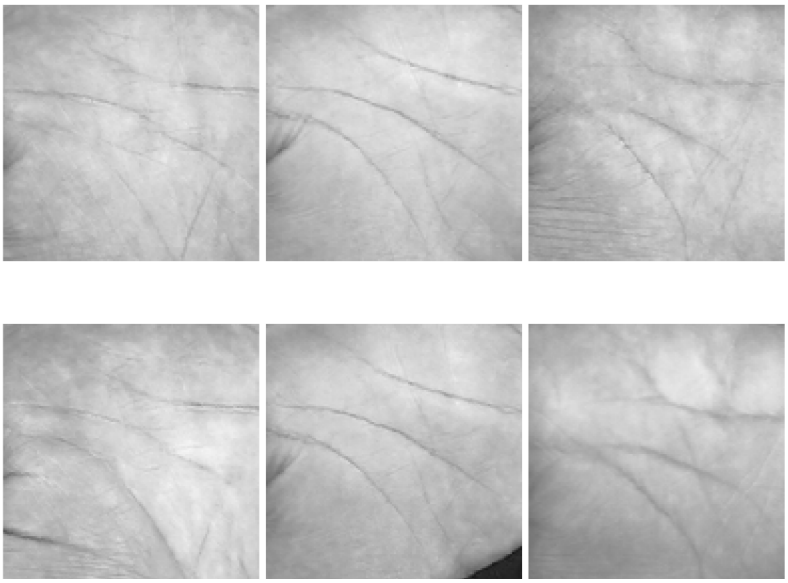

Figure 4. Some typical variations in the KTU palmprint database. The top and bottom images were taken from the same palm in various sessions. In the left, the image has been corrupted by incorrect placement of the hand. In the middle, clothes overlap the ROI. In the right, the hand was shifted and focus was changed.

Therefore, the database contains 1442 images from 153 different subjects. Of these, 612 images were used as the training set and 830 as the test set. From the real-life experiments, 601 palmprint images were also collected from 184 different people who did not have any sample in the training set. Some of them were obtained from users who did not complete the enrollment task. The other images were also captured from biometric attacks realized by unregistered users during the real-world applications. This is a good collection to get a novel database that can be used for more realistic tests. Those 601 images can be utilized in the imposter matchings for offline experiments.

Most of the studies in the literature have used palmprint databases acquired in laboratory conditions. In laboratory conditions, usually, there is a human administrator who tells the users what to do. This can be an unrealistic situation to develop a useful online system for daily usage. Furthermore, the images collected in laboratory conditions can be far from real-world conditions. As another novel work in this paper, the database acquisition was achieved in real-world conditions. In other words, simultaneous to the online palmprint system operation over 3 months, the images were automatically collected from individuals who used the system to enter the PC laboratory.

5.2. PolyU palmprint database

This database [3] was acquired by collecting 7752 images from 386 different palms using a palmprint capture device in laboratory conditions. The images were collected in two sessions. The first ten samples were captured in the first session and the other ten were regularly collected in the second session. The average interval between two sessions was 69 days. The resolution of original palmprint images is 384 $\times$ 284 pixels.

5.3. Experimental results

We present the results for the palmprint recognition and verification experiments on both the KTU and PolyU palmprint databases. In the recognition case, the system is first trained with the patterns that have known

labels. For each person, a biometric template is calculated in the training stage. Then the system assigns the test pattern to the person with the most similar template. In the verification case, a person's identity is claimed as a priori. The verified pattern is compared with the person's individual template only. It is checked whether the similarity between pattern and template is sufficient to provide access to the secured system. Generally, recognition rates are presented to show the recognition performance. In the literature, the palmprint verification performances are usually given by EER value and ROC graph [1].

5.3.1. Experiments on KTU palmprint database

Off-line palmprint recognition and verification experiments were performed on the KTU palmprint database acquired from the real-life palmprint verification application. In the recognition studies, the first 4 samples for each person (totally 612 images) were chosen as the training set. The rest of the samples (830 images) were used as the test set. To observe the contribution of the number of training samples to recognition performance, we used 2, 3, and 4 images for each person as training samples. Recognition results for different feature extraction methods are given in Table 1, comparatively. The number of images in the test set for each person varies between 2 and 16. The numbers given in Table 1 indicate recognition accuracies (%) and number of features.

Table 1. Recognition rates (%) of the methods/number of features with increased number of training samples in the KTU palmprint database.

No. training samples per class / feature extraction method	PCA	KPCA	FLD	KFD
2	87.83 / 200	90.60 / 269	93.01 / 153	96.02 / 153
3	90.24 / 200	94.10 / 403	96.27 / 153	97.83 / 153
4	94.10 / 320	96.39 / 527	98.55 / 153	99.16 / 153

The results show that kernel approaches (KPCA and KFD) gave better performance than linear approaches (PCA and FLD). Furthermore, the performance of the FLD is superior to that of PCA.

Another point to be noted is that the number of features for the FLD-based approaches is lower than for the PCA-based approaches and remains the same with different number of training samples. This situation arises from the difference between those two methods' problem-solving strategies. In the FLD-based approaches, because the 1vsA output coding scheme was used, the numbers of features are equal to the numbers of classes. On the other hand, in the PCA-based approaches, the numbers of features are related to the total training samples. From Table 1, it can be also seen that the recognition performance is improved by increasing the number of training samples.

The weighted Euclidean distance (WED)-based nearest neighbor (NN) classifier, used in the experiments, is compared with some other distances (Euclidean, Manhattan, cosine) and classifiers (k-NN with different k values, support vector machines (SVMs) with different kernels) in Table 2 to reveal the success of the selected method.

Table 2. Performance comparison of the classification methods on the KTU palmprint database.

Class. method:	NN + WED	NN + Euclid.	NN + Manhattan	NN + Cosine	k-NN (k = 3.5)	SVM (linear)	SVM (Polyn)	SVM (RBF)
Recog. rate:	99.16	98.80	99.04	98.80	99.04	98.80	98.80	99.16

From the results in Table 2, it can be seen that NN+WED and SVMs with radial basis function (RBF) kernel gives superior results than the others. However, the WED-based NN method can be preferred because the SVM method has high computational overhead.

In the experiments, the cumulative match scores were also computed. The resultant rank curve is given in Figure 5. The proposed method gives 99.16%, 99.64%, and 99.88% accuracies for rank 1, 3, and 8, respectively. The 99.88% recognition rate achieved in rank-8 indicates that only one test sample was unrecognized in the first eight predictions.

To obtain the system verification results, each test sample was matched with all training samples. If the two samples are from the same palm, the matching is marked as correct matching; otherwise it is marked as incorrect matching. In the verification experiments, performed on the KTU database, the test samples were collected from both users who completed the enrollment task and unregistered users who did not have any sample images in the training set. Therefore, the test set has totally 1431 images collected from 337 individuals: 830 images from 153 individuals and 601 images from 184 unregistered users.

Consequently, the test set contains more individuals than the training set. The total number of matchings is 875,772. The correct matching number is 3320, and the incorrect matching number is 872,452. The false acceptance rate (FAR) and false reject rate (FRR) curves for the proposed method were estimated by correct and incorrect matchings and are shown in Figure 6. Figure 6 also shows the effect of enlarging the database with the samples gathered from the unregistered users. In the graphic, the FAR-extended curve is generated using all test samples, while the FAR curve is generated by using samples captured from the registered users only. The overlapping area between the FAR-extended and FRR curves is bigger than the area between the FAR and FRR curves, which causes lower but more realistic performance results. Hereafter we use the extended FAR curve for the verification experiments.

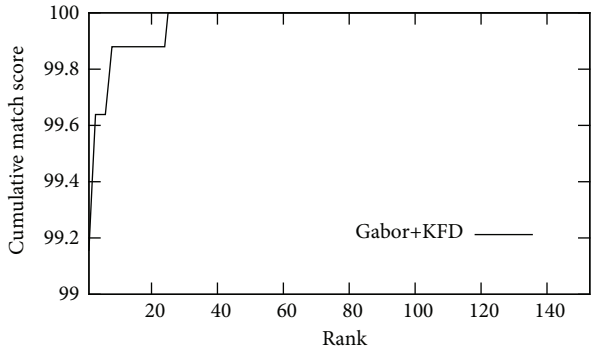

Figure 5. Cumulative match scores for the proposed method on the KTU database.

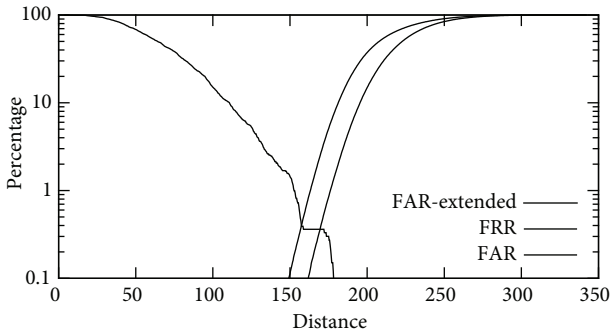

Figure 6. Logarithmic FAR-FRR curves of the proposed method on the KTU database.

The standard receiver operating characteristics (ROC) graph, which is plot of genuine acceptance rate (1-FRR) against false acceptance rate, is mostly used in the literature to show the performance of biometric recognition algorithms. Figure 7 shows the ROC curves generated from four different approaches (Gabor-based PCA, KPCA, Fisher linear discriminant (FLD), and KFD) implemented on the KTU database. According to the ROC curves, the KFD method is better than the other three approaches. The weakness of the PCA-based methods appears in the verification experiments. For small values of FAR, the PCA- and KPCA-based methods gave poor performance.

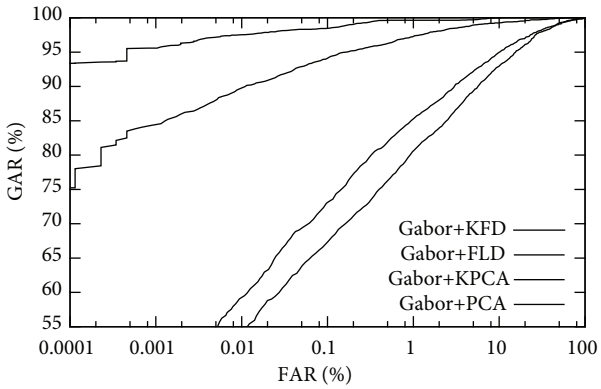

Figure 7. ROC curves of the proposed method and other methods.

Some performance criterion values achieved by different Gabor-based approaches (PCA, KPCA, FLD, and KFD) performed on the KTU database are summarized in Table 3. We can also see that the KFD approach can operate with a 93.193% genuine acceptance rate and a 0.0001% false acceptance rate. The system's equal error rate (EER) is 0.396%. In the EER values, the KFD method's advantage is evident. Only 0.396% error was achieved by the KFD method, while the other methods gave higher error rates.

Table 3. Verification results (%) of the methods on the KTU palmprint database.

	PCA	KPCA	FLD	KFD
GAR (when FAR = 1E-4%)	23.072	23.765	74.819	93.193
EER	8.048	6.649	1.942	0.396

The average time taken to execute each step can be summarized as follows: preprocessing: 94 ms, Gabor wavelets: 93 ms, KFD feature extraction: 145 ms, matching 1 ms. The total verification time is approximately 0.3 s. It can be obviously seen from the execution times that the system is considerably fast.

5.3.2. Experiments on PolyU database

To compare the proposed algorithm with recently published works, we performed similar experiments on the early PolyU palmprint database [3]. This database contains two versions. The first version contains 600 gray scale images captured from 100 different palms. Six samples from each palm were collected in two sessions, where three images were captured in the first session and the other three in the next session. We did not need to perform the experiments on this database, because we achieved 100% recognition accuracy in our previous work [16]. Therefore, the performances of some works such as [18,21], which were obtained on the previous PolyU database, are not discussed in the comparison section. In this work, the second version of the PolyU database, which is detailed in section 5.2, was utilized.

In the experiments on the second version of the PolyU database (commonly used in recent works), the images collected in the first session were considered as the training set, and the second session images were chosen as test images. To obtain the verification results, totally 14,784,000 incorrect matchings and 38,500 correct matchings were done. Figure 8 depicts the FAR-FRR and ROC graphs obtained with our method.

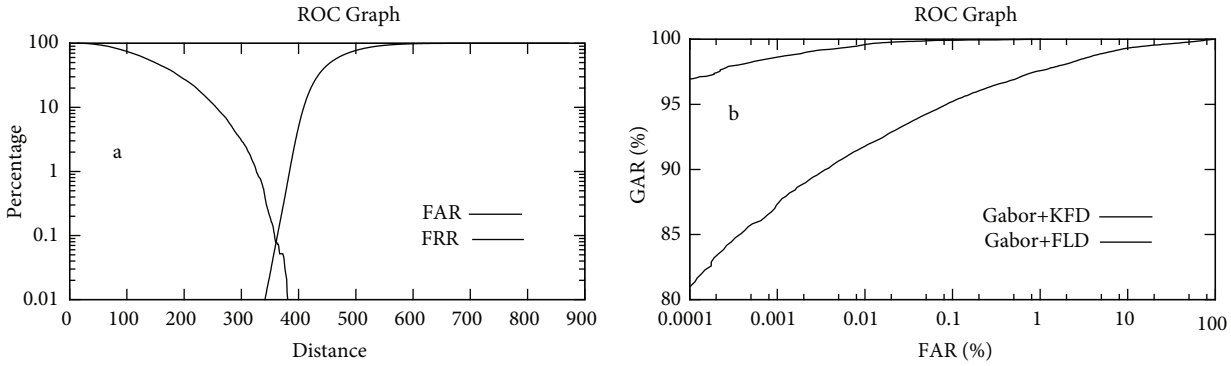

Figure 8. a) Logarithmic FAR-FRR curves of the Gabor-based KFD method, b) ROC curves of the Gabor-based FLD and KFD methods on the PolyU palmprint database.

Numerical results for the verification and recognition experiments on the PolyU database are summarized in Table 4. With the proposed method, a high recognition rate (99.714%) and low EER value (0.078%) were achieved. Genuine acceptance rate when FAR is equal to 1E-4% is 96.945%. Another remarkable point in Tables 3–5 is that the kernel methods gave better results than the linear methods.

Table 4. Recognition and verification results (%) of the Gabor-based FLD and KFD methods on the PolyU palmprint database.

	FLD	KFD
Recognition rate	98.961	99.714
GAR (when FAR = 1E-4%)	80.988	96.945
EER	1.926	0.078

Finally, Tables 5 and 6 summarize the comparison results between the proposed method and recent published works. For consistency, only the papers in which similar experiments were performed on the same database were considered. Although our method gives better results than the most popular coding approaches (PalmCode (0.7% EER), CompCode (0.43% EER), OrdinalCode (0.89% EER) etc.), we did not take them into account for the comparisons, because their results were achieved by matching the palmprint images acquired within the same session. In contrast, we matched the palmprints acquired within the second session with the palmprint images captured in the first session. This scheme demonstrates a more realistic scenario regarding the consideration of many distortions.

As shown in Table 5, the performance of the proposed algorithm is very competitive and higher than that of the other approaches. In the proposed work, 10 images collected in the first session for each palm were used as the training set; 3850 images corresponding to 385 different palms were also selected for testing. The early works [10,28–31] given in Table 5 also used first session images as the training set and the rest of the images as the test set. In [11], unlike the others, they used 2000 images of 100 different palms although the database contains 7752 images of 386 different palms. Furthermore, they selected 3 images per individual for the training set, and the rest of the database was used for the test set although each session includes 10 images.

Table 5. Comparison of different palmprint recognition methods on the PolyU-II database.

	Proposed method	In [30] 2009	In [31] 2008	In [10] 2009	In [32] 2010	In [33] 2009	In [11] 2008
Recog. rate (%)	99.714	98.0	99.15	97.22	97.13	96.82	95.71

Table 6. Comparison of different palmprint verification methods on the PolyU-II database.

	Proposed method	In [34] 2007	In [35] 2009	In [9] 2008	In [36] 2008	In [10] 2009	In [37] 2011
EER (%)	0.078	0.086	0.129	0.16	0.565	0.982	1.0

Some published works have also presented their experimental results for palmprint verification only. To show the performance of the proposed algorithm for palmprint verification, the recent published palmprint verification algorithms were comparatively illustrated in Table 6. The performances of the approaches given in Table 6 were also achieved with the same scenario on the PolyU palmprint database. In other words, the images collected in the first session were chosen as the training set, while the palms captured in the second session were used as the test set to achieve the biometric verification accuracies. As seen from Table 6, the presented method also gave better performance (0.078% EER) than other recent published algorithms implemented within a similar scenario.

6. Conclusion

We have presented a method to authenticate the identity of users based on nonlinear biometric palmprint features. This method has been performed on a CCD camera-based online palmprint verification system employed as an access controller in a real office environment. The user utilized the system without help from a human administrator. In other words, the enrollment and verification tasks were automatically accomplished under the control of the system. For this goal, user-friendly interface software was also developed to give instructions to the subjects for using the system and for placing their hands into platform in order to easily extract the ROI of the palm. In parallel with the online system operation over 3 months, the palmprint samples collected from the real-life applications were saved in a database. This database may become the first palmprint database acquired from palmprint biometric applications in real-world conditions.

To achieve a nonlinear biometric palmprint feature representation, a novel Gabor-based kernel Fisher discriminant analysis (KFD) method by the integration of the Gabor wavelet representation of palm images and the KFD method was proposed for online palmprint verification. All steps in the proposed method were coded in C++ programming language and then adapted into the novel online palmprint verification system. This system was then deployed in a student PC laboratory for a door opening system over three months. This is also one of the contributions in this paper. Unfortunately, most of the published works have coded their algorithms by using MATLAB libraries and achieved their results on databases acquired in laboratory conditions. In laboratory conditions, usually there is a human administrator who tells the users what to do.

Furthermore, experimental results were also achieved on the KTU palmprint database containing images collected from real-life biometric applications explained in this paper, in contrast to laboratory conditions. The proposed approach achieved an equal rate of 0.396% on this database including 2043 images from 337 different persons. As a novel experimental study in this paper, 612 palm images collected from 153 individuals were used as the training set and totally 1431 palmprint images were chosen as the test set; 830 images in the test set were acquired from persons who did not have any images in the training set.

For comparison of the performance of the proposed algorithm with the recent published papers, the experimental results on the palmprint recognition and verification were also performed on the PolyU palmprint database commonly used in the literature. The performance of the proposed algorithm is very competitive (0.078% EER and 99.714% recognition rate) and at least one of the best algorithms among recent palmprint verification and recognition algorithms.

Acknowledgment

The work described in this paper has been fully supported by the National Science Foundation under Project No. 107E212. The authors are grateful for the constructive advice and comments from the anonymous reviewers.

References

[1] Zhang D, Xiaoyuan J, Jian Y. Biometric Image Discrimination Technologies (Computational Intelligence and Its Applications Series). 2006; Hershey, PA, USA: Idea Group Publishing.

[2] Connie T, Jin ATB, Ong MGK, Ling DNC. An automated palmprint recognition system. Image Vision Comput 2005; 23: 501-515.

[3] Zhang D, Kong WK, You J, Wong M. Online palmprint identification. IEEE T Pattern Anal 2003; 25: 1041-1050.

[4] Kumar A. Incorporating cohort information for reliable palmprint authentication. In: IEEE 2008 6th Indian Conference on Computer Vision, Graphics & Image Processing; 16–19 December 2008; Bhubaneswar, INDIA: IEEE. pp. 583-590.

[5] Sun Z, Tan T, Wang Y, Yunhong L, Stan Z. Ordinal palmprint representation for personal identification. In: IEEE 2005 Conference on Computer Vision and Pattern Recognition; 20–25 June 2005; San Diego, CA, USA: IEEE. pp. 279-284.

[6] Boles WW, Chu SYT. Personal identification using images of the human palm. In: IEEE 1997 Region 10 Annual Conference on Speech and Image Technologies for Computing and Telecommunications; 2–4 December 1997; Brisbane, Australia: IEEE. pp. 295-298.

[7] Jia W, Huang DS, Zhang D. Palmprint verification based on robust line orientation code. Pattern Recogn 2008; 41: 1504-1513.

[8] Noh JS, Rhee KH. Palmprint identification algorithm using Hu invariant moments and Otsu binarization. ICIS 2005 4th Annual International Conference on Computer and Information Science; 14–16 July 2005; Jeju Isl, South Korea: pp. 94-99.

[9] Aykut M. Ekinci M. Kernel principal component analysis of Gabor features for palmprint recognition. In IAPR/IEEE 2009 3rd International Conference on Advances in Biometrics; 02-05 June 2009; Alghero, Italy: IAPR; IEEE. pp. 685-694.

[10] Yan Y, Zhang YJ. Discriminant projection embedding for face and palmprint recognition. Neurocomputing, 2008; 71: 3534-3543.

[11] Kittler J, Hatef M, Duin R, Matas J. On Combining Classifiers. IEEE T Pattern Anal 1998; 20: 226-239.

[12] Zhang D, Zuo W, Yue F. A Comparative Study of Palmprint Recognition Algorithms. ACM Comput Surv 2012; 44: 2:1-37.

[13] Mika S, Ratsch G, Weston GJ, Scholkopf B, Mullers KR. Fisher discriminant analysis with kernels. In IEEE 1999 Workshop on Neural Networks for Signal Processing IX; 23-25 August 1999; Madison, WI, USA: IEEE. pp. 41-48.

[14] Ekinci M. KTU-CVPR Palmprint Database Version 1, Available at: http://ceng.ktu.edu.tr/∼cvpr/palmDB1.htm.

[15] Pan X, Ruan QQ. Palmprint recognition using Gabor feature-based (2D)2PCA. Neurocomputing 2008; 71: 3032-3036.

[16] Ekinci M, Aykut M. Gabor-based kernel PCA for palmprint recognition. Electron Lett 2007; 43: 1077-1079.

[17] Laadjel M, Bouridane A, Kurugollu F, Yan WQ. Palmprint recognition based on subspace analysis of Gabor filter bank. International Journal of Digital Crime and Forensics 2010; 2: 1-15.

[18] Wu X, Zhang D, Wang K. Fisherpalms based palmprint recognition. Pattern Recogn Lett 2003; 24: 2829-2838.

[19] Savic T, Pavesic N. Personal recognition based on an image of the palmar surface of the hand. Pattern Recogn 2007; 40: 3152-3163.

[20] Wang Y, Ruan Q. Kernel Fisher discriminant analysis for palmprint recognition. IAPR 2006 18th International Conference on Pattern Recognition, ICPR '06; 20–24 August 2006, Hong Kong: IAPR. pp. 457-460.

[21] Laadjel M, Bouridane A, Kurugollu F, Boussakta S. Palmprint recognition using Fisher-Gabor feature extraction. In: IEEE 2008 Int. Conf. on Acoustics, Speech and Signal Processing, 30 March–04 April 2008; Las Vegas, NV, USA: IEEE. pp. 1709-1712.

[22] Otsu N. A threshold selection method from gray-level histograms. IEEE T Syst Man Cyb 1979; 9: 62-66.

[23] Sonka M, Hlavac V, Boyle R. Image Processing, Analysis, and Machine Vision, 2nd ed. Toronto, Canada: PWS Publisher, 1999, pp. 142-147.

[24] Daugman JG. Uncertainty relation for resolution in space, spatial frequency, and orientation optimized by two-dimensional visual cortical filters. J Opt Soc Am A 1985; 2: 1160-1169.

[25] Daugman JG. Complete discrete 2-D Gabor transforms by neural networks for image analysis and compression. IEEE T Acoust Speech 1988; 36: 1169-1179.

[26] Weldon TP, Higgins WE, Dunn DF. Efficient Gabor filter design for texture segmentation. Pattern Recogn 1996; 29: 2005-2015.

[27] Liu C. Gabor-based kernel PCA with fractional power polynomial models for face recognition. IEEE T Pattern Anal 2004; 26: 572-581.

[28] Mika S, Ratsch G, Muller KR. A mathematical programming approach to the kernel Fisher algorithm. 14th Annual Neural Information Processing Systems Conference; 27 November–02 December 2000, Denver, CO, USA: pp. 591-597.

[29] Zhu Y, Tan T, Wang Y. Biometric personal identification based on handwriting. In: IEEE 15th Int. Conf. on Pattern Recognition; 03–07 September 2000, Barcelona, Spain: IEEE. pp. 2797-2800.

[30] Lu J, Zhao Y, Hu J. Enhanced gabor-based region covariance matrices for palmprint recognition. Electron Lett 2009; 45: 880-881.

[31] Wei J, Huang DS, Dacheng T, Zhang D. Palmprint identification based on directional representation. In: IEEE 2008, Int. Conf. on Systems, Man and Cybernetics; 12–15 October 2008; Singapore: IEEE: pp. 1562-1567.

[32] Hu RX, Wei W, Huang DS, Lei YK. Maximum margin criterion with tensor representation. Neurocomputing 2010; 73: 1541-1549.

[33] Shen L, Ji Z, Zhang L, Guo Z. Applying LBP operator to Gabor response for palmprint identification. In: IEEE 2009, Int. Conf. on Information Engineering and Computer Science; 19–20 December 2009; Wuhan, Hubei, China; IEEE: pp. 1-3.

[34] Hennings-Yeomans PH, Kumar BVKV, Savvides M. Palmprint classification using multiple advanced correlation filters and palm-specific segmentation. IEEE T Inf Foren Sec 2007; 2: 613-622.

[35] Zhu YH, Jia W, Liu LF. Palmprint recognition using band-limited phase-only correlation and different representations. In: IEEE 2009 5th international conference on Emerging intelligent computing technology and applications; 16–19 September 2009, Ulsan South Korea: IEEE. pp. 270-277.

[36] Huang DS, Jia W, Zhang D. Palmprint verification based on principal lines. Pattern Recogn 2008; 41: 1316-1328.

[37] Badrinath G, Kachhi N, Gupta P. Verification system robust to occlusion using low-order Zernike moments of palmprint sub-images. Telecommun Syst 2011; 47: 275-290.